Synthesis, Characterization, and Second-Order Optical Nonlinearity of a Polyurethane Structure Functionalized with a Hemicyanine Dye

Ki-Jeong Moon and Hong-Ku Shim*

Department of Chemistry, Korea Advanced Institute of Science and Technology, Taejon 305-701, Korea

Kwang-Sup Lee*

Department of Macromolecular Science, Han Nam University, Taejon 300-791, Korea

Jaroslaw Zieba and Paras N. Prasad*

Photonics Research Laboratory, Department of Chemistry, State University of New York at Buffalo, Buffalo, New York 14260-3000

Received March 3, 1995; Revised Manuscript Received November 1, 1995[⊗]

ABSTRACT: A new polyurethane structure with a hemicyanine dye attached to the polymer side chain was synthesized by the step growth polymerization in a reaction between (*E*)-*N*-butyl-4-[2-[4-[bis(2-hydroxyethyl)amino]phenyl]ethenyl]pyridinium tetraphenylborate and 2,4-toluene diisocyanate. The molecular weight of the final product was determined to be $M_n = 12\,000$ and $M_w/M_n = 1.67$. The polymer is soluble in dimethylformamide and can be processed into optical quality films by spin casting. No evidence of melting was detected by differential scanning calorimetry, suggesting that this polymer presents an amorphous phase. It shows a glass transition temperature of 121 °C. The macroscopic second-order hyperpolarizability $\chi^{(2)}$ of this polyurethane was determined by measuring the second harmonic generation (SHG) for a thin polymer film. The $\chi^{(2)}$ value was in the range 1.8×10^{-7} to 5.0×10^{-7} esu, depending upon poling conditions. This high second-order activity seems to prove the earlier prediction about a possible enhancement in the nonlinear second-order properties of organic materials triggered by utilizing the strong electron-accepting nature of the pyridinium group. In the presented polymer, the alignment of the nonlinear chromophore moieties induced by electric poling exhibits an extended temporal stability, due to the stabilizing function of the hydrogen bridges formed between the neighboring polyurethane chains, preventing the relaxation of oriented molecular dipoles.

Introduction

Nonlinear optics is drawing steady attention because of its wide application proposed in the photonics-based technologies of optical signal processing, optical switching, optical sensing, etc. A wide variety of materials including inorganic and organic crystals, thin films, and organic polymers and polymeric composites possess nonlinear optical (NLO) properties.[1−3] Among them, the polymeric materials processed into thin films are expected to play an important role mainly because of the high optical nonlinearity, high optical damage threshold, fast response times, flexibility of chemical and structural modification, and ease of processing.[4]

In second-order optically nonlinear materials, generally, the NLO active chromophores are incorporated either by doping or by attaching via covalent bonds to an amorphous polymer[5,6] or a liquid crystalline polymer.[7] In addition to these dye-doped and side chain NLO systems, two other classes of polymeric materials have been proposed. In the first one, the NLO units are incorporated into a polymer backbone.[8] In the second one, a rigid polymeric structure with uniformly oriented NLO chromophore molecules is obtained by thermally or photochemically induced cross-linking reactions.[9]

In organic polymer based optically second-order active nonlinear materials, noncentrosymmetric alignment of the NLO chromophore molecules needs to be introduced by applying high dc electric fields at temperature close to the polymer glass transition, producing the macroscopic second-order optical nonlinearity. However, the molecular dipoles of the NLO chromophore tend to randomize their orientation after the electric field is removed, since the process of electric field poling brings the system off its equilibrium. This, in turn, principally causes a decay in the observed macroscopic second-order nonlinearity of a given material. Two approaches to minimize the randomization have been proposed. In the first approach, a high T_g polymer (such a polyimide) is blended with an NLO chromophore, producing a material with enhanced temporal and thermal stability.[10] In the second approach, a main chain NLO polymer is combined with a thermally or photochemically cross-linkable chemical unit.[11] Yet, these two methods present some drawbacks. In the high T_g "host−guest" systems, the doping level of the polymeric matrix with the NLO chromophore is limited either by its possible recrystallization or by its plasticizing effect which significantly lowers the glass transition temperature of the host polymer when added in higher concentrations. Additionally, even high molecular weight molecules tend to sublime from the polymer layer, since poling sometimes requires temperatures above 200 °C. This sublimation lowers the effective doping level, resulting in a decrease of the macroscopic second-order hyperpolarizability $\chi^{(2)}$. In the cross-linkable systems, optical losses are significant, caused by the limited uniformity of the cross-linking reaction.

In order to circumvent these problems we have developed a polyurethane structure with covalently linked side chain moieties containing a highly active

[⊗] Abstract published in *Advance ACS Abstracts,* December 15, 1995.

0024-9297/96/2229-0861$12.00/0

NLO chromophore. The main reason we select the polyurethane as a matrix is that an extensive formation of hydrogen bonds between the urethane linkage is expected to increase the rigidity of the matrix and to prevent the randomization process of the oriented NLO chromophore dipoles. Moreover, the structure we propose in this work presents a high degree of saturation of the polymer with an optically second-order active chromophore, reaching 68% (by weight). On the other hand, in the part of our work devoted to the material design we decided to take advantage of the high second-order susceptibility of hemicyanine moieties.[12] It is well-known that in this class of NLO chromophores their nonlinear activity is strongly dependent upon the properties of the anion and it usually increases when big, "softer" anions are used.[13] Thus, we have chosen, as the counterion for the hemicyanine chromophore, the bulky tetraphenylborate anion. This, beyond the increase in nonlinear activity of the chromophore, was expected to reduce the ion mobility in the strong electric field during the poling process and slow down the process of relaxation of aligned molecular dipoles after removal of the electric field.

In this paper we report the synthesis and the physicochemical and optical characterization of this new polyurethane structure. We discuss the details of its optical second-order activity in terms of electric field poling and temporal and thermal stability.

Experimental Section

Materials. *N*,*N*-Dimethylformamide (DMF) (Junsei) was purified by distillation under reduced pressure over anhydrous magnesium sulfate and dried further over a molecular sieve. 2,4-Toluene diisocyanate (Aldrich) was purified by distillation under reduced pressure. All other solvents and reagents were used without further purification.

Monomer Synthesis. [*N*,*N*-Bis(hydroxyethyl)amino]benzene (1). A mixture of 177 g (2.2 mol) of 2-chloroethanol, 93 g (1.0 mol) of aniline, and 91.6 g (2.2 mol) of 96% sodium hydroxide was stirred at 100 °C for 3 days. The mixture was cooled to room temperature, extracted with methylene chloride and washed with water. The organic layer was dried with anhydrous magnesium sulfate, concentrated, and purified by recrystallization with diethyl ether/petroleum ether. The product yield was 157.7 g (87%). Mp: 55−56 °C. ^{1}H-NMR ($CDCl_3$): δ 7.2 (m, 2H, Ar H3 and H5), 6.7 (m, 3H, Ar 2H, H4 and H6), 4.5 (s, 2H, OH), 3.7 (t, 4H, J = 4.5 Hz, $N(CH_2CH_2\text{-}OH)_2$), 3.5 (t, J = 4.5 Hz, 4H, $N(CH_2CH_2OH)_2$). IR (KBr pellet, cm^{-1}): 3200−3600 (OH), 1598 and 1504 (Ar CH). Anal. Calcd for $C_{10}H_{15}NO_2$: C, 66.27; H, 8.34; N, 7.73. Found: C, 65.90; H, 8.38; N, 7.43.

[*N*,*N*-Bis[(acetyloxy)ethyl]amino]benzene (2). To a solution of 26.0 g (0.14 mol) of compound **1** in 200 mL of methylene chloride were added 43.9 g (0.43 mol) of acetic anhydride and 32 g (0.40 mol) of pyridine, and the resulting mixture was refluxed. After 1 day, the reaction mixture was cooled and washed with water. The organic layer was dried with anhydrous magnesium sulfate and then concentrated. The product was purified by vacuum distillation to give a yellow viscous oil of 31.6 g (83%). Bp: 182 °C/1.2 mmHg. ^{1}H-NMR ($CDCl_3$): 7.2 (m, 2H, Ar H3 and H5), 6.8 (m, 3H, Ar H2, H4 and H6), 4.3 (t, 4H, J = 6.2 Hz, $N(CH_2CH_2OAc)_2$), 3.6 (t, 4H, J = 6.2 Hz, $N(CH_2CH_2OAc)_2$, 2.1 (s, 6H, $OCOCH_3$). IR (NaCl, cm^{-1}): 1738 (C═O), 1599 and 1505 (Ar CH), 1241 (C−O). Anal. Calcd for $C_{14}H_{19}NO_4$: C, 63.38; H, 7.22; N, 5.28. Found: C, 63.00; H, 7.27; N, 5.25.

4-[*N*,*N*-Bis[2-(acetyloxy)ethyl]amino]benzaldehyde (3). Anhydrous DMF (40 mL) was placed in a flask and was cooled in ice bath. Then 25.4 g (0.17 mol) of phosphorus oxychloride was added dropwise with stirring. After 30 min, 40 g (0.15 mol) of compound **2** was added to the flask. The solution was heated at 90 °C for 2 h. The reaction mixture was then cooled, poured over crushed ice in a beaker, and neutralized to pH 6−8 by dropwise addition of saturated sodium acetate solution. The mixture was extracted with ethyl acetate. The extracts were washed with water, dried with magnesium sulfate, and then concentrated. The residue was purified by column chromatography to yield 42.2 g (96%) of **3** as a yellow solid. Mp: 60 °C. ^{1}H-NMR ($CDCl_3$): δ 9.7 (s, 1H, CHO), 7.7 (d, 2H, J = 8.9 Hz, Ar H2 and H6 to CHO), 6.8 (d, 2H, J = 8.9 Hz, Ar H3 and H5 to CHO), 4.2 (t, 4H, J = 6.2 Hz, $N(CH_2CH_2OAc)_2$), 3.7 (t, 4H, J = 6.2 Hz, $N(CH_2CH_2OAc)_2$), 2.0 (s, 6H, $OCOCH_3$). IR (KBr pellet, cm^{-1}): 1736 and 1660 (C═O), 1594 and 1527 (Ar, CH), 1241 (C−O). Anal. Calcd for $C_{15}H_{19}NO_5$: C, 61.42; H, 6.53; N, 4.78. Found: C, 61.11; H, 6.61; N, 4.68.

***N*-Butyl-γ-picolinium Bromide (4).** A mixture of 18 g (0.19 mol) of 4-picoline, 26.5 g (0.19 mol) of *n*-butyl bromide, and 120 mL of acetonitrile was heated at 80 °C for 1 day. After removal of the solvent, 39.4 g (90%) of hydroscopic solid **4** was produced. Mp: 135.5 °C. ^{1}H NMR (D_2O): δ 9.3 (d, 2H, J = 6.2 Hz, Py H2 and H6 to N$^+$), 7.7 (d, 2H, J = 6.2 Hz, Py H3 and H5 to N$^+$), 4.7 (t, 2H, J = 7.4 Hz, $N^+CH_2CH_2CH_2CH_3$), 2.5 (s, 3H, CH_3), 1.8 (m, 2H, $N^+CH_2CH_2CH_2CH_3$), 1.2 (m, 2H, $N^+CH_2CH_2CH_2CH_3$), 0.8 (t, 3H, $N^+CH_2CH_2CH_2CH_3$). IR (KBr pellet, cm^{-1}): 3200−3600 (adsorbed H_2O), 1640 and 1470 (Ar CH and CN). Anal. Calcd for $C_{10}H_{16}NBr$: C, 52.19; H, 7.01; N, 6.06. Found: C, 51.49; H, 7.03; N, 5.88.

(*E*)-*N*-Butyl-4-[2-[4-[bis(2-hydroxyethyl)amino]phenyl]ethenyl]pyridinium Bromide (5). To a solution of 6.15 g (0.027 mol) of **4** and 8.24 g (0.028 mol) of **3** in 100 mL of methanol was added a catalytic amount of 0.5 mL of piperidine, and then the mixture was refluxed. After 2 days, methanol was evaporated and a small portion of acetone was added. Scratching of the residue by a spatula gave a red solid. This solid was washed with acetone several times. The yield was 6.96 g (59%). Mp: 87−90 °C. ^{1}H-NMR (D_2O): δ 8.1 (d, 2H, J = 6.2 Hz, Py H2 and H6 to N$^+$), 7.6 (d, 2H, J = 6.2 Hz, Py H3 and H5 to N$^+$), 7.3 (m, 3H, Ar H3 and H5 to $N(CH_2CH_2OH)_2$ and CH═$CHArN(CH_2CH_2OH)_2$), 6.6 (m, 3H, Ar H2 and H6 to $N(CH_2CH_2OH)_2$ and CH═CHAr$N(CH_2CH_2OH)_2$), 4.0 (t, 2H, $N^+CH_2CH_2CH_2CH_3$), 3,7 (t, 4H, $N(CH_2CH_2OH)_2$), 3.5 (t, 4H, $N(CH_2CH_2OH)_2$), 1.7 (m, 2H, $N^+CH_2CH_2CH_2CH_3$), 1,2 (m, 2H, $N^+CH_2CH_2CH_3$), 0.8 (t, 3H, $N^+CH_2CH_2CH_2CH_3$). IR (KBr pellet, cm^{-1}): 3200−3600 (OH), 1584 and 1519 (Ar C═C), 820 (Ar CH). Anal. Calcd for $C_{21}H_29N_2O_2Br$: C, 59.86; H, 6.94; N, 6.65. Found: C, 59.12; H, 7.10; N, 6.53.

(*E*)-*N*-Butyl−4-[2-[4-[bis(2-hydroxyethyl)amino]phenyl]ethenyl]pyridinium Tetraphenylborate (6). To a solution of 10 g (0.024 mol) of **5** in 200 mL of methanol was added dropwise a solution of 8.1 g (0.024 mol) of sodium tetraphenylborate in 200 mL of methanol. A red precipitate was formed immediately. The precipitate was collected by filtration and then dried. The product yield was 12.4 g (78%). Mp: 76−77 °C. ^{1}H-NMR (DMSO-d_6): δ 8.7 (d, 2H, J = 6.7 Hz, Py H2 and H6 to N$^+$), 7.9 (d, 2H, J = 6.7 Hz, Py H3 and H5 to N$^+$), 7.8 (d, 1H, J = 16 Hz, CH═$CHArN(CH_2CH_2OH)_2$), 7.5 (d, 2H, J = 8.9 Hz, Ar H3 and H5 to $N(CH_2CH_2OH)_2$), 7.2−6.7 (m, 23H, Ar H2 and H6 to $N(CH_2CH_2OH)_2$, CH═CHAr$N(CH_2CH_2OH)_2$, and Ar H from $B(C_6H_5)_4^-$), 4.8 (t, 2H, OH), 4.4 (t, 2H, $N^+CH_2CH_2CH_2CH_3$), 3.5 (m, 8H, NCH_2CH_2OH), 1.8 (m, 2H, $N^+CH_2CH_2CH_2CH_3$), 1.3 (m, 2H, $N^+CH_2CH_2CH_2CH_3$), 0.9 (t, 3H, $N^+CH_2CH_2CH_2CH_3$). IR (KBr pellet, cm^{-1}): 3200−3600 (OH), 1580 and 1520 (Ar C═C), 830, 735, and 705 (Ar CH). UV/vis ($CHCl_3$): λ_{max} = 496 nm. Calcd for $C_{45}H_{49}N_2O_2B$: C, 81.81; H, 7.48; N, 4.24. Found: C, 81.10; H, 7.47; N, 4.33.

Polymer Synthesis. Polymer PU1-C4B. To a solution of 1.52 g (0.0023 mol) of compound **6** in 20 mL of anhydrous dimethylacetamide was gradually added 1 equiv of 2,4-toluene diisocyanate (TDI). The mixture was heated at 80 °C for 5 h while stirring. The reaction mixture was allowed to cool to room temperature and poured into cold water. A red precipitate was obtained, filtered, washed with water, and dried by vacuum. The polymer yield was 1.63 g (85%). ^{1}H-NMR (DMSO-d_6): δ 9.6 (br s, 1H, NHCO para to CH_3 from TDI), 8.9 (br s, 1H, NHCO ortho to CH_3 from TDI), 8.7 (m, 2H, py H2 and H6 to N$^+$), 7.9 (m, 3H, py H3 and H5 to N$^+$ and CH═$CHArN(CH_2CH_2O)_2$), 7.5 (m, 3H, Ar H3 and H5 to $N(CH_2CH_2O)_2$ and Ar H of TDI), 7.2−6.7 (m, 25H, Ar H from

$B(C_6H_5)_4^-$ and Ar H2 and H6 to $N(CH_2CH_2O)_2$ Ar H of TDI and CH=*CH*ArN$(CH_2CH_2OH)_2$), 4.3 (m, 6H, $N^+CH_2CH_2CH_2$-CH_3) and $N(CH_2CH_2O)_2$), 3.7 (br s, 4H, $N(CH_2CH_2O)_2$), 2.1 (br s, 3H CH_3 of TDI), 1.8 (m, 2H, $N^+CH_2CH_2CH_2CH_3$), 1.2 (m, 2H, $N^+CH_2CH_2CH_2CH_3$), 0.9 (t, 3H, $N^+CH_2CH_2CH_2CH_3$). IR (KBr pellet, cm^{-1}): 3100−3500 (NH), 1584 and 1519 (Ar C=C), 1720 (CO), 826, 735, and 705 (Ar CH). UV/vis (thin film): λ_{max} = 484 nm.

Measurements. The ^{1}H-NMR spectrum of the synthesized compound was recorded on a Bruker AM spectrometer. FT-IR spectra of the monomer and the polymer were obtained with a Bomem Michelson series FT-IR spectrophotometer. UV/vis absorption spectra were measured on a Shimadzu UV-3101PC spectrophotometer. Differential scanning calorimetry (DSC) and thermogravimetry were performed under nitrogen on a DuPont 9900 analyzer.

Thin polymer films were spin cast at spin rate ranging from 400 to 600 rpm from a 5.5% (by weight) solution of the polymer in a mixture of DMF and cyclopentanone (5:3 by weight) onto ITO-covered glass substrates. Prior to film casting the polymer solution was filtered through a 0.45 μm Teflon membrane filter (Aldrich). All films were dried for 2 h under reduced pressure at 80 °C to drive out the residual solvents.

Film thickness was determined using a Tencor Instruments Alpha-Step 100 profilometer. The thickness of films used in this work ranged between 0.7 and 1.3 μm. The refractive indices at the fundamental (1064 nm) and the second harmonic wavelengths for polymer films were obtained by combining the prism coupling technique which was used for measuring two refractive index values at 632.8 and 823 nm. The interference fringes method was used to determine the spectral dispersion of refractive indices in the range between 600 and 1550 nm. The refractive index of the polyurethane film at 1064 nm is 1.587, and it could be obtained directly from the spectral dispersion curve. The refractive index of 1.762 and 532 nm was estimated by extrapolation of the spectral dispersion curve, and thus its accuracy is limited by the strong contribution of the adsorption-related imaginary part.

The second harmonic generation experiments were performed with the p-polarized beam at the fundamental frequency of a mode-locked Q-switched Nd:YAG laser operating at 500 Hz with 40 135 ps subpulses in each pulse train. The optically nonlinear second-order activity of the polymer films was produced by using corona discharge induced electric poling. The poling was performed in a wire-to-plane geometry under *in situ* conditions.[14] This means that the ITO glass covered with the polymer film is positioned in a stage consisting of a massive copper plate with two cartridge heaters and a temperature monitoring system (a J type thermocouple connected to a CN6071A temperature controller, both from Omega Engineering, Inc.). The ITO layer and the copper plate are short-circuited. A single corona wire is expanded over the sample parallel to the film surface. The wire is electrically isolated from the copper plate. The "hot wire" from a high-voltage power supply is connected to the corona wire when its zero cable goes to the copper plate. The plate is positioned at the angle of about −45° to the incident IR laser beam which first passes through the polymer sample and then through a slitlike window in the copper plate and finally gets absorbed on an IR filter. The second harmonic radiation generated by the film is projected through a simple optical system onto an entrance window of a photomultiplier. Its signal is transferred to a data acquisition system. This design of our experimental setup allows us to observe the progress of poling by monitoring the changes in the second harmonic generation signal produced by the film through the entire process. Using this poling procedure, we could optimize the process parameters such as the intensity of the corona discharge, the distance between the film surface and the corona wire, and thus the effective poling field, the poling temperature, and time. In all our poling experiments we used the positive polarity of a 25 μm thick tungsten corona wire. The positive polarity was proven to work with our material more efficiently than the negative one. During the poling process the strength of the external dc electric field imposed across the polymer films was measured by using an electrostatic voltameter (Model 344, from

Scheme 1

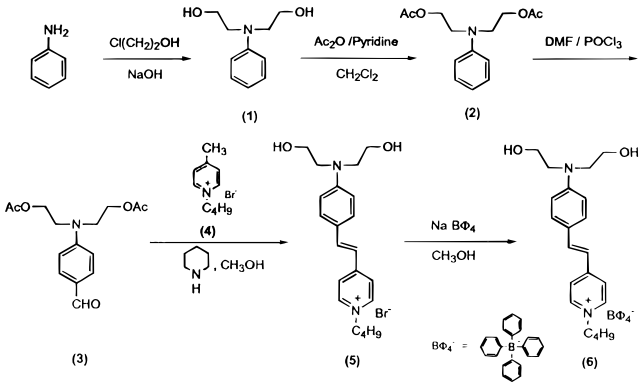

TREK Incorp.) which detects the voltage of the film surface produced by the corona discharge. Depending upon the ambient air humidity in our poling setup, the applied electric fields varied between 1.5×10^8 and 3.8×10^8 V m^{-1}. These fields were produced using a wire potential of +4.6 kV when the distance between the corona wire and the sample surface was around 0.60−0.63 cm. Every attempt to increase the corona wire voltage and to increase the poling efficiency caused uncontrolled corona discharge, resulting in damage of the poled film surface.

Typically, the poling was started by imposing the electric field across the polymer film at room temperature. In the next step the film was heated with a rate of 15−20 °C/min to 190 °C and kept at this temperature for a period of 60 min. We have not noticed any influence of the heating rate on the final results of the poling process. After 1 h of annealing at 190 °C, the film, with the electric field still on, was slowly brought back to room temperature. Finally, the electric field was removed.

The macroscopic second harmonic susceptibility $\chi^{(2)}$ of our films has been measured using the angular dependence method with a Y-cut quartz plate (d_{11} coefficient 0.81×10^{-10} esu) as the reference.[15]

Results and Discussion

Synthesis and Materials Characterization. The overall pathway of the monomer synthesis is presented in Scheme 1. In the first step, aniline was allowed to react with chloroethanol for 3 days under strongly basic conditions at 100 °C, yielding the diethanolamine derivative **1**. The hydroxyl group of compound **1** was then protected using acetic anhydride in pyridine. The aldehyde derivative **3** was obtained with a 96% yield by the Villsmeier formylation of **2**. A subsequent reaction of **3** with *N*-butyl-γ-picolinium bromide, which is derived from 4-picoline and *n*-butyl bromide, yielded 59% of the stilbazolium derivative **5**. Finally, monomer **6** was obtained by an ion exchange reaction between compound **5** and sodium tetraphenylborate. All intermediates, including the monomer, were characterized by common spectroscopic techniques such as IR, ^{1}H-NMR, UV/vis, and elemental analysis. Their results, presented in the Experimental Section, are in good agreement with the structures obtained in each stage of the synthetic route.

The polymerization of monomer **6** with 2,4-toluene diisocyanate is described in Scheme 2. The polyurethane (PU1-C4B), containing a salt type hemicyanine dye, was prepared by the step growth process in anhydrous DMF. The polymerization yield was 78%. The addition of dibutyltin dilaurate, as a catalyst, to the reaction mixture neither accelerated the polymerization reaction nor promoted the formation of higher molecular weight polymer chains. The molecular weight of our polyurethane structure, determined by GPC with

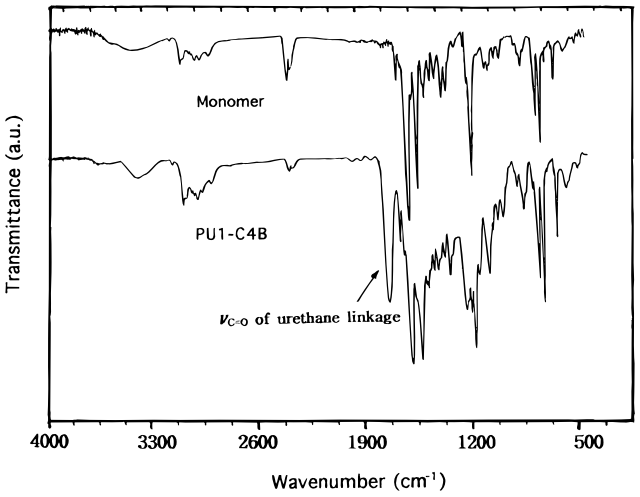

Figure 1. FT-IR spectra of monomer **6** and polyurethane PU1-C4B.

Scheme 2

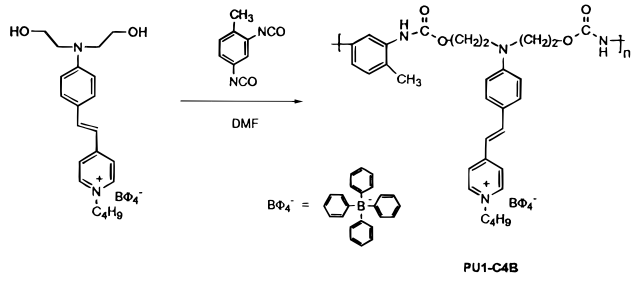

a polyurethane standard, was $M_n = 12\,000$ and $M_w/M_n = 1.67$. The polymer is readily soluble in DMF and its mixtures with cyclopentanone and cyclohexanone. From DMF/cyclopentanone solutions of PU1-C4B, excellent optical quality thin films can be cast on different glass substrates either by spin coating or by manual casting.

The polymer structure was characterized by IR, ^{1}H-NMR, and UV/vis absorption spectroscopy. As shown in Figure 1, the well-resolved peak of the stretching vibrations of the isocyanate group around 2300 cm^{-1} in the FT-IR spectrum of the polymer is very weak compared to the spectrum of the monomer and an equivalent amount of 2,4-toluene diisocyanate. At the same time the buildup of a strong peak at 1720 cm^{-1}, characteristic of the vibration of a carbonyl group, is apparent. These two facts indicate the formation of a urethane linkage, as proposed in Scheme 2. The ^{1}H-NMR data of the polyurethane in Figure 2 show a signal broadening due to polymerization, but the chemical shifts are consistent with the proposed polymer structure. The UV/vis absorption spectra of the monomer and the polymer are shown in Figure 3. The absorption maxima for the $\pi-\pi^*$ transition of the stilbene chromophore in **6** and PU1-C4B are at 496 and 484 nm, respectively. It means that the incorporation of the chromophore into the polyurethane chain causes a 12 nm blue shift in its intrinsic absorption, indicating an electronic interaction between the chromophore moiety and the polymer chain.

Thermal Properties. In Figure 4 a differential scanning thermogram of the PU1-C4B polymer, after its annealing at 190 °C for 1 h, is presented (temperature range 23−300 °C, heating rate 10 °C, nitrogen atmosphere). The DSC curve shows a clearly pronounced glass transition area starting at 121 °C. This T_g is higher than the glass transition temperature of

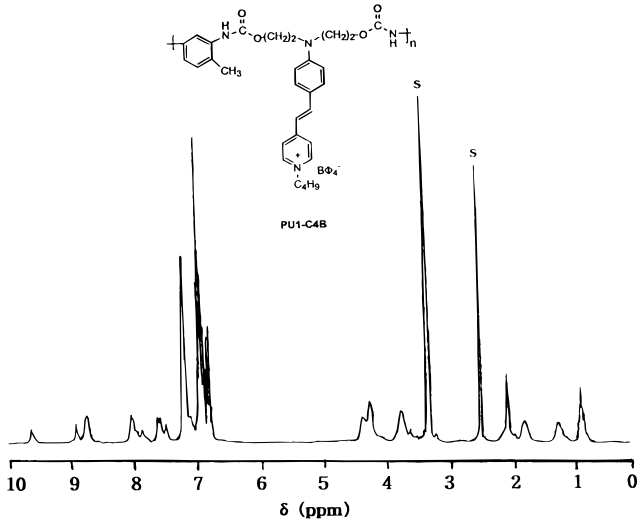

Figure 2. ^{1}H-NMR spectrum of PU1-C4B (in DMSO-d_6). Solvent signals are labeled as "s".

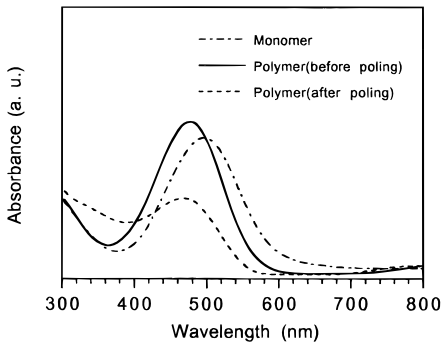

Figure 3. UV/vis absorption spectra of monomer **6** and polymer films on ITO-coated glass substrates before and after poling.

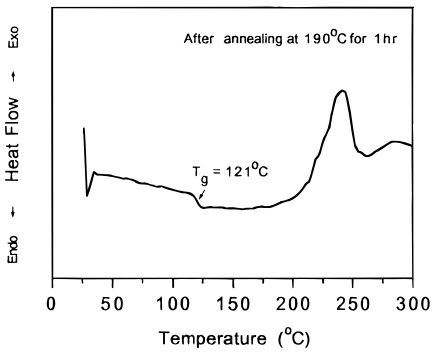

Figure 4. DSC thermogram of PU1-C4B (heating rate 10 °C/min).

common flexible polyurethanes. We attribute it to the enhanced rigidity of the polymer backbone in our system, caused by incorporation of the toluene rings. The presented DSC scan does not show any indication of the melting process, suggesting a noncrystalline phase of PU1-C4B. The second characteristic point on the DSC curve appears at about 220 °C, and it presents the temperature at which the thermal decomposition sets in. This value is slightly below what we obtained from a TGA analysis. We suspect this discrepancy to be caused by the difference in the heating rate we used in our experiments. In Figure 5 the thermal gravimetry scan (temperature range 25−1000 °C, heating rate 20 °C/min, nitrogen atmosphere) shows the onset of a weight loss at 225 °C. We assume that this first step in the thermal degradation process is related to the

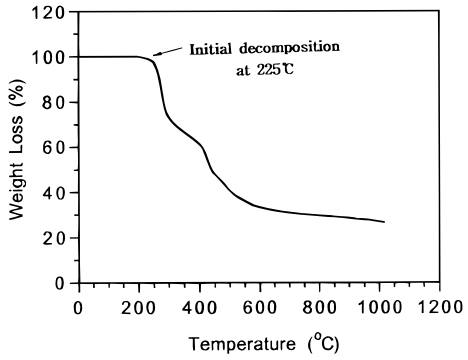

Figure 5. TGA scan data for PU1-C4B (heating rate 10 °C/min).

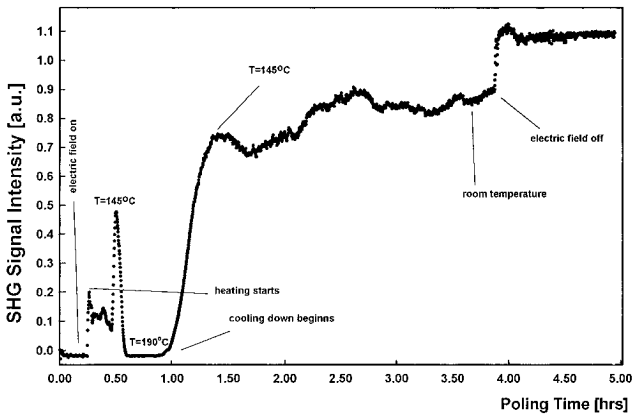

Figure 6. *In situ* scan profile obtained for ITO glass coated with PU1-C4B film.

decomposition of the tetraphenylborate group. This suggestion is supported by the fact that the calculated weight loss corresponds well with the fraction made by the molecular weight of the tetraphenylborate moiety in the overall molecular weight of the polymer structural unit.

Optically Nonlinear Properties of the PU1-C4B Polymer. A typical profile of our *in situ* poling experiments on the PU1-C4B polymer is shown in Figure 6. Directly after the poling field is imposed across the film at room temperature, a rapid buildup of the SHG signal is observed. In the next step the temperature is elevated. When it approaches 145 °C, a sharp increase in the SHG signal starts. It should be noted that in the temperature range between 20 and 145 °C no decrease was detected in the corona discharge produced electric potential on the film surface. However, it starts to decrease when the temperature is elevated further. This drop in the sample surface potential is associated with a pronounced decay in the SHG signal intensity. When the sample temperature reaches 190 °C, its surface potential is almost zero and so is the SHG intensity. It suggests that at temperatures above 145 °C the electrical conductivity of the polymer appears. This was confirmed by a separate experiment in which we measured the dark current flowing through a PU1-C4B film as a function of temperature.

After a temperature of 190 °C was reached, the sample was allowed to anneal for 1 h. The high-temperature curing step appears to improve the temporal stability of the once introduced alignment of the hemicyanine chromophore. The annealing time of 1 h was set arbitrarily. After annealing at this temperature, down step of the poling experiment began. Almost immediately, after the temperature was lowered to

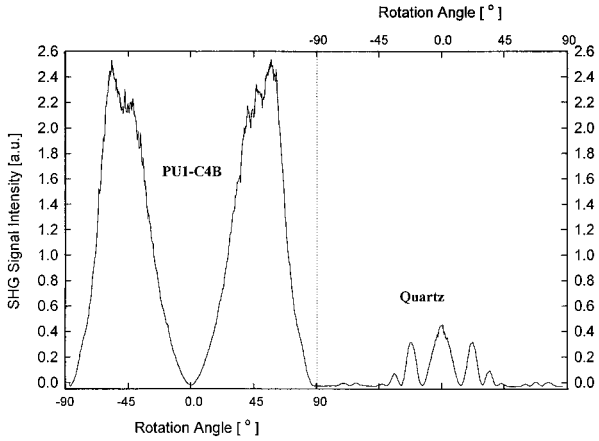

Figure 7. Angular dependence of a 0.7 μm thick, poled PU1-C4B film compared with the signal of a 1 mm thick Y-cut quartz plate.

about 170 °C, a recovery of the SHG signal was observed. At the same time we began to see an increase in the sample surface potential.

A more rapid increase in the SHG intensity was obtained until the temperature reached 145 °C. The same applies to the electric surface potential. In the temperature range between 145 °C and room temperature, the signal increase was slower. When the sample reached room temperature, the electric field was removed. The electric surface potential of the sample discharged rapidly to zero and, at the same time, a fast rise in the SHG signal intensity occurred. A possible explanation can be based on the assumption that the dipole moment vector and the largest component of the β tensor are not colinear. In such a situation it is conceivable that a reorientation after the poling field is removed may lead to a more favorable projection to produce enhanced $\chi^{(2)}$. However, this observation needs further detailed study for a better understanding.

In order to determine the macroscopic second-order susceptibility $\chi^{(2)}$ of the material, the sample was removed from the poling stage after poling was completed. Its angular SHG dependence was recorded and then compared with the values obtained from a 1 mm thick, Y-cut quartz plate (see Figure 7). After optimizing the poling conditions, we were able to produce, with good reproducibility, second-order active PU1-C4B films with a $\chi^{(2)}$ value of 3×10^{-7} esu. It should be noted that the electric poling process changes the spectral properties of the polyurethane films. For comparison, a spectrum, recorded after the poling process was accomplished, is presented in Figure 3. It can be seen that, compared with the spectrum of the same film before poling, the absorption decreased significantly. This effect is partially reversible, and the absorption increases when the dipole alignment is randomized. This type of behavior for poled films is well-known and is explained in terms of processes present in electroabsorption.[16] Additionally, it cannot be excluded that, because of the extended annealing process at 190 °C, a partial thermal decomposition of the chromophore may have taken place during poling.

In Figure 8 the temporal stability of the nonlinear activity of a poled PU1-C4B film is presented. The second harmonic generation signal of a poled film, stored at room temperature, was recorded periodically over a period of 33 days. The decay in the value of the SHG signal is negligible within experimental error. This result shows an excellent temporal stability of chro-

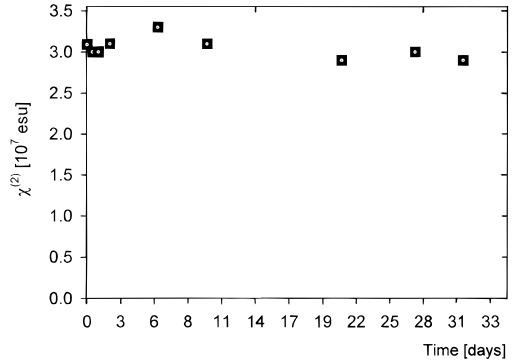

Figure 8. Temporal stability of poling alignment at room temperature.

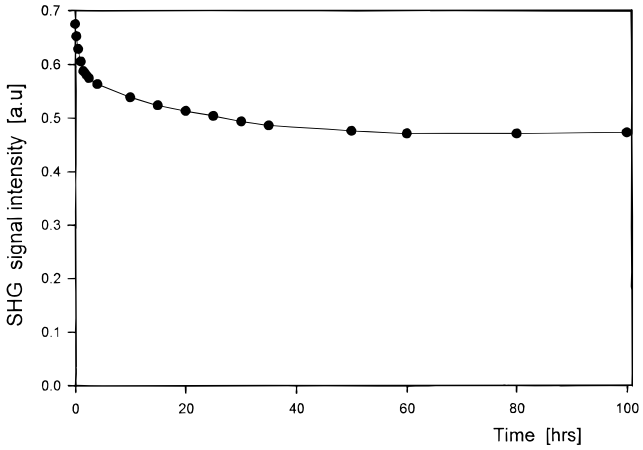

Figure 9. Temporal stability of poling alignment at 100 °C.

mophore alignment in our polyurethane structure. The high $\chi^{(2)}$ value of our system and its time profile support our earlier expectations regarding both the enhanced second-order nonlinearity and an extended temporal stability of suitably designed NLO polymers with organic salt containing chromophores.[17]

Moreover, as shown in Figure 9, the material still retains almost 70% of its initial optically nonlinear activity after being exposed for 100 h to the temperature of 100 °C. Indeed, as we pointed out at the beginning, the improvement in the temporal stability was expected because of the extensive formation of hydrogen bridges between neighboring polymer chains which, in turn, was anticipated to increase the matrix rigidity. The stability is often associated with the intermolecular bonding. It was shown that in a cross-linked system the decay in temporal stability is minimized,[9] while weak intermolecular bonding shows rapid and large decay.[5,6] In our system since the the stability is maintained and since hydrogen bridges in polyurethane, polyamide, polypeptide, etc. are well-known and documented, the observed stability in our system can be attributed to the hydrogen bond formation.[18−20] In addition since this polymer was shown to be completely amorphous, the high entropy conformation of the backbone chain allows the hydrogen bonding to take place, even in the presence of bulky NLO side groups. Thus when our system is compared with other systems such as poly(methyl methacrylate) or polystyrene-based NLO polymers, where the hydrogen bonding does not occur,[6] a better stability can be obtained, as was shown.

Though the T_g of 121 °C is lower than the values reported for many other NLO materials, we want to hypothesize that considering the very high loading ratio

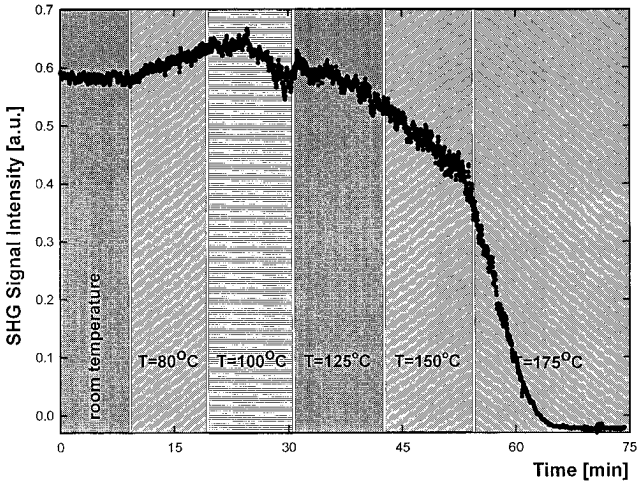

Figure 10. Thermal stability of poling alignment in PU1-C4B.

of our material with the chromophore, the glass transition temperature should be considered as relatively high. If one considers that 26% doping with a lophine chromophore lowers the T_g of an isotropic poly(ether imide) from 220 to 150 °C, then a further increase in lophine concentration to the level we propose in our system will cause an additional drop in the T_g of this polyimide-based material.[21]

Next, we monitored the thermal endurance of its SHG activity. In this experiment the SHG signal was monitored every 10 min under stepwise increasing temperatures. The result is presented in Figure 10. It can be clearly seen that at the temperature near 125 °C the SHG signal starts to decrease slowly. The rate with which the SHG signal decreases does not change significantly when the temperature is increased to 150 °C. This is consistent with the DSC data we presented in Figure 4, in which the quite broad region of the glass transition process, reaching beyond 150 °C, is apparent. Furthermore, when the temperature reaches 175 °C, a fast signal decay sets in, causing the SHG signal to disappear within 10 min. This depoling process is irreversible and the SHG signal does not recover when the sample is brought back to room temperature.

Conclusion

A new type of an NLO active, hemicyanine dye substituted polyurethane was prepared. It shows a high second-order optically nonlinear activity and good temporal and thermal stabilities. The *in situ* poling profile shows that a new feature of this material triggers a significant increase in the observed SHG value immediately after the electric poling field is removed. A stable, good reproducible value of the macroscopic second-order susceptibility $\chi^{(2)}$ on the order of 3×10^{-7} esu was obtained.

Acknowledgment. This research was supported by the Korea Science & Engineering Foundation (KOSEF) and the Air Force Office of Scientific Research, Directorate of Chemical Sciences, through contract number F49620-93-C0017. We thank Makoto Yoshida for his help in determining the refractive indices of our films.

References and Notes

(1) Marder, S. R.; Sohn, J. E.; Stucky, G. D. *Materials for Nonlinear Optics: Chemical Perspective*; ACS Symposium Series 455; American Chemical Society: Washington, DC, 1991.

(2) Chemla, D. S.; Zyss, J. *Nonlinear Optical Properties of Organic Molecules and Crystals*; Academic Press: Orlando, FL, 1987.
(3) Prasad, P. N.; Williams, D. J. *Introduction to Nonlinear Optical Effects in Molecules and Polymers*; John Wiley: New York, 1991.
(4) Lee, K.-S.; Samoc, M.; Prasad, P. N. In *Comprehensive Polymer Science*; Aggarwal, S. L., Russo, S., Eds.; Pergamon Press: Oxford, U.K., 1992; 1st Suppl. Vol.
(5) (a) Singer, K. D.; Shon, J. E.; Lalama, S. J. *Appl. Phys. Lett.* **1986**, *49*, 248. (b) Hampsch, H. L.; Yang, J.; Wong, G. K.; Torkelson, J. M. *Macromolecules* **1990**, *23*, 3640.
(6) (a) Ye, C.; Marks, T. J.; Yang, J.; Wong, G. K. *Macromolecules* **1987**, *20*, 2322. (b) Yoshida, M.; Asano, M.; Tamada, M.; Kumakura, M. *Makromol. Chem., Rapid Commun.* **1989**, *10*, 517.
(7) (a) Noel, C.; Friedrich, C.; Leonard, V.; LeBarny, P.; Ravaux, G.; Dubois, J. C. *Makromol. Chem., Macromol. Symp.* **1989**, *24*, 283. (b) Yitzchaik, S.; Berkovic, G.; Krongauz, V. *Macromolecules* **1990**, *23*, 3539. (c) Robello, D. R. *J. Polym. Sci., Polym. Chem. Ed.* **1990**, *28*, 1. (d) Wijekoon, W. M. K. P.; Zhang, Y.; Karna, S. P.; Prasad, P. N.; Griffin, A. C.; Bhatti, A. M. *J. Opt. Soc. Am. B* **1992**, *9*, 1832.
(8) (a) Green, G. D.; Weinschenk, J. I.; Mulvaney, J. E.; Hall, H. K., Jr.; *Macromolecules* **1987**, *20*, 722. (b) Willand, C. S.; Williams, D. J. *Ber. Bunsenges. Phys. Chem.* **1987**, *91*, 1304. (c) Katz, H. E.; Schilling, M. L. *J. Am. Chem. Soc.* **1989**, *111*, 7554. (d) Xu, C.; Wu, B.; Dalton, L. R.; Ranon, P. M.; Shi, Y.; Steier, W. H. *Macromolecules* **1992**, *25*, 6716. (e) Francis, C. V.; White, K. M.; Newmark, R. A.; Stephens, M. G. *Macromolecules* **1993**, *26*, 4379. (f) Wright, M. E.; Mullick, S. *Macromolecules* **1992**, *25*, 6045.
(9) (a) Eich, M.; Reck, B.; Yoon, D. Y.; Willson, C. G.; Bjorkland, G. C. J. *Appl. Phys.* **1989**, *66*, 3241. (b) Hubbard, M. A.; Marks, T. J.; Yang, J.; Wong, G. K. *Chem. Mater.* **1989**, *1*, 167. (c) Mandal, B. K.; Kumar, J.; Huang, J. C.; Tripathy, S. K. *Makromol. Chem., Rapid Commun.* **1991**, *12*, 63. (d) Hayashi, A.; Goto, Y.; Nakayama, M.; Sato, H.; Watanabe, T.; Miyata, S. *Macromolecules* **1992**, *25*, 5094. (e) Jeng, R. J.; Chen, Y. M.; Chen, J. I.; Kumar, J.; Tripathy, S. K. *Macromolecules* **1993**, *26*, 2530. (f) Ranon, R. M.; Shi, Y.; Steier, W. H.; Xu, C.; Wu, B.; Dalton, L. R. *Appl. Phys. Lett.* **1993**, *62*, 2605. (g) Boogers, J. A. F.; Klaase, P. Th. *A.*; de Vlieger, J. J.; Alkema, D. P. N.; Tinnemans, A. H. A. *Macromolecules* **1994**, *27*, 197. (h) Boogers, J. A. F.; Klaase, P. Th. A.; de Vlieger, J. J.; Tinnemans, A. H. A. *Macromolecules* **1994**, *27*, 205.
(10) Stähelin, M.; Walsh, C.; Burland, D.; Miller, R.; Twieg, R.; Volksen, W. *J. Appl. Phys.* **1993**, *73*, 8471.
(11) Ranon, P. M.; Shi, Y.; Steier, W. H.; Xu, C. H.; Dalton, L. R. *Organic Thin Films for Photonics Application*, OSA, 1993, Technical Digest Series Volume 17; p 10.
(12) Laidlaw, W. M.; Denning, R. G.; Verbiest, T.; Chauchard, E.; Persoons, A. *Nature* **1993**, *363*, 58.
(13) Ashwell, G. J.; Hargreaves, R. C.; Baldwin, C. E.; Bahra, G. S.; Brown, C. R. *Nature* **1992**, *357*, 393.
(14) Zieba, J.; Zhang, Y.; Cassteans, M.; Burzynski, R.; Prasad, P. N. *Proc. SPIE—Int. Soc. Opt. Eng.* **1992**, *1758*.
(15) Saleh, B. E. A.; Teich, M. C. *Fundamentals of Photonics*; John Wiley and Sons, Inc.: New York, 1991; p 780.
(16) Burland, D. M.; Miller, R. D.; Walsh, C. A. *Chem. Rev.* **1994**, *94* (1), 31.
(17) Choi, D. H.; Kim, H. M.; Wijekoon, W. M. K. P.; Prasad, P. N. *Chem. Mater.* **1992**, *4* (6), 1255.
(18) Lin, S. B.; Hwang, K. S.; Tsay, S. Y.; Cooper, S. L. *Colloid Polym. Sci.* **1985**, *263*, 128.
(19) Bonart, R. *J. Macromol. Sci., Phys.* **1968**, *B2* (1), 115.
(20) Seymour, R. B. *Polymer Chemistry*; 2nd ed.; Marcel Dekker: New York, 1988; p 175.
(21) Stähelin, M.; Walsh, C.; Burland, D.; Miller, R.; Twieg, R.; Volksen, W. *J. Appl. Phys.* **1993**, *73*, 8471.

MA950275C